

29. Adhesive Behavior of Polycaprolactone review 1.docx

by Cek Turnitin

Submission date: 16-Sep-2025 09:45PM (UTC-0500)

Submission ID: 2753326838

File name: 29._Adhesive_Behavior_of_Polycaprolactone_review_1.docx (787.58K)

Word count: 6646

Character count: 40398

Adhesive Behavior of Polycaprolactone/Hydroxyapatite Coatings on 316L Stainless Steel: A Design of Experiments Approach

Agung Prabowo^{1*}, Ahmad Fadli², Heni Sugesti³, Muh Irwan⁴, Syarifuddin Oko⁵, Gading Bagus Mahardika⁶, Marlinda⁷

^{1,4,5,6,7} Chemical Engineering Department, Politeknik Negeri Samarinda, Samarinda, 75131, East Kalimantan, Indonesia

² Chemical Engineering Department, Engineering Faculty, Universitas Riau, Pekanbaru, 28293, Riau, Indonesia

³ Chemical Engineering Department, Politeknik Negeri Sriwijaya, Palembang, South Sumatra, Indonesia

*email : agungprabowo@polnes.ac.id

Article History

Received: XX XXXXXXX XXX; Received in Revision: XX XXXXXXX XXX; Accepted: XX XXXXXXX XXX

Abstract

Enhancing the adhesive strength of bioactive coatings is crucial for improving the mechanical stability of metallic implants. This study investigates the effects of three processing parameters—sonication temperature (X_1), PCL/HA ratio (X_2), and drying time (X_3)—on the adhesive strength of poly(ϵ -caprolactone)/hydroxyapatite (PCL/HA) composite coatings applied to 316L stainless steel substrates. A full factorial 23 experimental design was employed, and the results were analyzed using analysis of variance (ANOVA) and regression modeling. The adhesive strength response ranged from 19.62 MPa to 63.27 MPa. Among the factors studied, the PCL/HA ratio had the most significant positive effect, while drying time showed a minor influence. Interaction plots and response surface analyses revealed a synergistic effect between sonication temperature and PCL/HA ratio, contributing to improved bonding at the coating-substrate interface. The optimization results yielded a predicted maximum adhesive strength of 25.76 MPa at a desirability score of 0.03, highlighting the complexity of parameter interactions. These findings underscore the importance of processing conditions in tailoring coating performance for biomedical applications.

Keywords: PCL/HA composite coatings, Adhesive strength, 316L stainless steel, Factorial design, Optimization.

Abstrak

Meningkatkan kekuatan adhesi lapisan bioaktif sangat penting untuk memperbaiki stabilitas mekanik pada implan logam. Penelitian ini menyelidiki pengaruh tiga parameter proses—suhu sonikasi (X_1), rasio PCL/HA (X_2), dan waktu pengeringan (X_3)—terhadap kekuatan adhesi lapisan komposit poli(ϵ -kaprolakton)/hidroksiapatit (PCL/HA) yang diaplikasikan pada substrat baja tahan karat 316L. Desain eksperimen faktorial penuh 2^3 digunakan, dan hasilnya dianalisis menggunakan analisis varians (ANOVA) serta pemodelan regresi. Respon kekuatan adhesi berkisar antara 19,62 MPa hingga 63,27 MPa. Di antara faktor-faktor yang diteliti, rasio PCL/HA memberikan pengaruh positif paling signifikan, sedangkan waktu pengeringan menunjukkan pengaruh yang relatif kecil. Plot interaksi dan analisis permukaan respon menunjukkan adanya efek sinergis antara suhu sonikasi dan rasio PCL/HA, yang berkontribusi pada peningkatan ikatan pada antarmuka lapisan-substrat. Hasil optimasi menghasilkan kekuatan adhesi maksimum prediksi sebesar 25,76 MPa dengan skor desirabilitas 0,03, yang menyoroti kompleksitas interaksi parameter. Temuan ini menegaskan pentingnya kondisi proses dalam menyesuaikan kinerja lapisan untuk aplikasi biomedis.

Keywords: Lapisan komposit PCL/HA, Kekuatan adhesi, Baja tahan karat 316L, Desain faktorial, Optimasi.

1. Introduction

316L stainless steel (SS 316L) is a prominent candidate in the field of temporary bone implant materials due to its favorable attributes, including corrosion resistance, mechanical

strength, and cost-effectiveness (Haleem et al., 2024; Aroussi et al., 2019). Within the broader classification of metallic biomaterials, such as cobalt-chromium alloys and titanium-based constructs, SS 316L is noted for its excellent mechanical properties, including high fatigue resistance, which are critical for orthopedic applications (Haleem et al., 2024; Aroussi et al., 2019). However, the biologically inert nature of SS 316L limits its long-term success due to inferior osseointegration, which can jeopardize implant durability (Fadli, 2021; Luo et al., 2018). Such limitations necessitate the exploration of bioactive coatings aimed at enhancing the material's interaction with bone tissue. Hydroxyapatite (HA) coatings emerge as a leading solution, given HA's chemical and structural resemblance to natural bone mineral (Singh et al., 2023; Ielo et al., 2022). HA fosters osteoblast adhesion and proliferation and can enhance the corrosion resistance of the underlying metallic substrate, potentially improving the implant's integration in vivo (Homa et al., 2024; Ielo et al., 2022). The structural properties of HA reveal a hexagonal lattice with parameters $a = 9.432 \text{ \AA}$ and $c = 6.881 \text{ \AA}$, giving it specific characteristics beneficial for biological applications (Vasudev & Prakash, 2023). Despite the promising bioactivity attributed to HA, it has limitations; its mechanical brittleness and insufficient tensile strength can hinder its utility in weight-bearing orthopedic implants (Saputra et al., 2021; Ielo et al., 2022).

To overcome the mechanical limitations of hydroxyapatite (HA) coatings, considerable research has focused on developing composite systems that incorporate polymers to improve both structural integrity and long-term performance (Ramesh et al., 2018). Among the various candidates, poly(ϵ -caprolactone) (PCL) has garnered significant attention due to its favorable mechanical properties, excellent biocompatibility, and biodegradability (Taghizadeh et al., 2024; Uler et al., 2011; Sowmya et al., 2021). PCL is a semi-crystalline aliphatic polyester that undergoes slow hydrolytic degradation under physiological conditions, yielding non-toxic by-products that can be readily metabolized or excreted by the body. These characteristics make PCL highly suitable for biomedical applications such as drug delivery, tissue engineering scaffolds, and implant coatings (Gunatillake & Adhikari, 2003).

However, PCL on its own lacks the osteoconductivity and cellular adhesion properties essential for orthopedic coatings (Liang et al., 2024). To address this, the combination of PCL with HA in a polymer-ceramic composite offers a promising approach—providing the mechanical flexibility and processability of the polymer while preserving the bioactivity of the ceramic component (Monia & Ridhal., 2024). In this study, PCL/HA composite coatings were synthesized and applied to 316L stainless steel (SS 316L) substrates using a dip-coating technique. This low-temperature process eliminates the need for sintering, thereby preserving the mechanical integrity of the underlying metal while enabling uniform coating deposition.

The primary aim of this work was to evaluate the effect of PCL concentration and ultrasonic processing temperature on the mechanical adhesion strength of the composite coating. A two-level full factorial design (2k) was implemented to assess the influence and interaction of processing variables on coating performance. Shear strength testing was conducted to quantify the adhesion between the composite layer and the metallic substrate, serving as a direct measure of mechanical stability. Analysis of Variance (ANOVA) was employed to identify the most statistically significant factors affecting coating adhesion. The results highlight the critical role of optimizing both the polymer-ceramic ratio and the processing conditions to achieve coatings with enhanced interfacial adhesion and mechanical robustness. These improvements position the optimized PCL/HA composite coatings as strong candidates for orthopedic applications requiring durable, load-bearing implant surfaces.

2. Methodology

Materials

Stainless steel 316L plates (30 × 20 × 3 mm) were used as substrates. The surfaces were polished with 1200 grit SiC paper, then cleaned in acetone (Merck) using an ultrasonic bath for 15 minutes, dried, and stored in a desiccator. For pretreatment, the substrates were immersed in 5 M sodium hydroxide (NaOH, Merck) at 60°C for 24 hours, dried at 80°C for 1 hour, and sintered at 600°C for 1 hour. Poly(ϵ -caprolactone) (PCL) pellets and hydroxyapatite (HA) powder were purchased from Sigma-Aldrich (UK) and used without further purification. Acetone (Merck) was used as the solvent for slurry preparation.

Pretreatment of SS 316L

A stainless steel 316L (SS 316L) plate with dimensions of 30 × 20 × 3 mm was employed as the metallic substrate. Prior to coating deposition, the substrates were mechanically polished using silicon carbide (SiC) abrasive paper with a grit size of 1200 to remove surface contaminants and

Commented [r1]: Add the chemical formula of PCL.

enhance surface roughness for improved coating adhesion. Following mechanical treatment, the samples were ultrasonically cleaned in acetone for 15 minutes to eliminate residual impurities, then dried and stored in a desiccator to prevent surface oxidation. To further investigate the influence of ultrasonic processing temperature and alkali pretreatment on the surface characteristics of SS 316L, an additional surface modification step was introduced. The polished substrates were immersed in 50 mL of 5 M NaOH aqueous solution and maintained at 60°C for 24 hours to induce chemical surface activation. After alkali treatment, the samples were dried using warm airflow at 80°C for 1 hour, followed by a sintering process at 600°C for 1 hour. This thermal treatment aimed to stabilize the modified surface morphology and enhance the interfacial adhesion properties of the subsequent coating.

Preparation of PCL/HA Slurry and Coating Deposition on SS 316L
Poly(ϵ -caprolactone) (PCL) pellets and hydroxyapatite (HA) powder, both obtained from Sigma-Aldrich (England), were used as received without further purification. To prepare the composite coating solution, PCL pellets (20–40 wt.%) were dissolved in acetone at room temperature under continuous magnetic stirring. Once the PCL was fully dissolved, HA powder was gradually introduced into the solution and stirred for 24 hours at room temperature to ensure homogeneous dispersion of HA particles within the PCL matrix. The coating process was conducted using a dip-coating technique at room temperature. SS 316L substrates were vertically immersed in the PCL/HA suspension and withdrawn at a constant speed to achieve uniform film deposition. Following coating, the samples were dried in an oven at 60°C for either 10 or 14 hours to evaluate the effect of drying duration on the mechanical and electrochemical properties of the composite coatings.

Characterization Techniques

The adhesive strength of the PCL/HA composite coating on SS 316L substrates was evaluated using a universal testing machine (Instron 5569). Prior to testing, the uncoated side of each specimen was mechanically roughened by sandblasting to ensure consistent surface texture and promote effective bonding. This surface was then bonded to an aluminum rod using a triethanolamine-based epoxy resin [$N(CH_2CH_2OH)_3$]. After the initial bonding, the samples underwent thermal curing in a drying oven at 110°C for 24 hours. To ensure uniform stress distribution during testing, the coated surface of each specimen was similarly bonded to a flat aluminum plate using the same adhesive and curing protocol. The assembled specimens were mounted on the testing apparatus, and tensile shear tests were conducted at a constant crosshead speed of 1 mm/min. The test was continued until coating delamination or failure occurred. The maximum load recorded prior to failure was used to calculate the shear adhesive strength of the PCL/HA composite coating.

Experimental Design

To systematically investigate the influence of key processing parameters on the properties of PCL/HA composite coatings, a full factorial design of experiments (2^3) was utilized. This statistical approach allowed for the evaluation of both main effects and interaction effects among the selected variables. The independent variables considered in this study were: PCL concentration (20 wt.% and 40 wt.%), ultrasonic treatment temperature (45°C and 55°C), and drying time (10 hours and 14 hours). These factors were tested at two levels—low and high—as summarized in Table 1. The factorial design provided a structured and efficient framework for analyzing how these parameters influence the mechanical and electrochemical performance of the coatings, particularly with respect to shear bond strength. Through systematic variation of the input variables, the study aimed to determine the optimal processing conditions to enhance coating adhesion and stability.

Table 1. Factors and their levels

Levels	Sonication Temperature (°C)	PCL/HA Ratio (%wt)	Substrate and composite drying time (hours)
High (1)	55	40	14
Low (-1)	45	20	10

In this design, 8 factorial points performance tests were conducted. Table 2 shows the experimental plan and the obtained results for this design.

Commented [r2]: Add the flowchart on pretreatment of SS 316L.

3

Table 2. Experimental plan and results for 2^k factorial design.

No.	Sonication Temperature (°C)	PCL/HA Rasio (%wt)	Substrate composite and drying time (hours)	Coded Variables			Response Adhesive strength (MPa)
				X ₁	X ₂	X ₃	
1	45	20	10	-1	-1	-1	10.61
2	45	20	14	-1	-1	1	1.73
3	45	40	10	-1	1	-1	42.15
4	45	40	14	-1	1	1	15.75
5	55	20	10	1	-1	-1	11.01
6	55	20	14	1	-1	1	33.88
7	55	40	10	1	1	-1	29.59
8	55	40	14	1	1	1	61.36

55

3. Results and Discussion (Capital, Bold, Verdana 9, initial letter)

Commented [r3]: typo

The successful deposition of poly(ϵ -caprolactone)/hydroxyapatite (PCL/HA) composite coatings onto SS 316L substrates was confirmed through a combination of morphological, structural, and phase characterization techniques. Initial visual inspection revealed smooth, continuous coatings without visible defects, indicating uniform film formation across the substrate surface. This uniformity is attributed to the synergistic effects of sonication-assisted dispersion, optimized PCL/HA ratio, and controlled drying time, which together enhanced coating homogeneity and interfacial adhesion. As illustrated in Figure 1, the adhesion mechanism of the PCL/HA composite coating to the SS 316L surface involves both chemical and electrostatic interactions. The naturally occurring passive oxide layer on stainless steel introduces surface hydroxyl ($-OH$) groups, which facilitate hydrogen bonding with the carbonyl ($C=O$) groups of the PCL polymer chains (Hetemi & Pinson, 2019). Concurrently, hydroxyapatite particles are embedded within the polymer matrix and anchored to the substrate via electrostatic interactions. Specifically, calcium ions (Ca^{2+}) and phosphate groups (PO_4^{3-}) participate in ionic bonding with surface species on the oxide layer, contributing to the mechanical stability and bioactivity of the coating (Drevet et al., 2019).

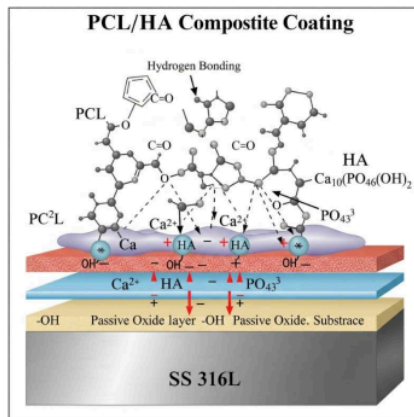


Figure 1. Schematic illustration of the interfacial interactions between the PCL/HA composite coating and the SS 316L substrate. The passive oxide layer on stainless steel promotes hydrogen bonding with PCL chains, while HA particles are immobilized via electrostatic interactions involving Ca^{2+} and phosphate (PO_4^{3-}) groups.

53

Ultrasonic treatment during the preparation of the PCL/HA composite coating plays a critical role in enhancing the dispersion of hydroxyapatite particles within the polymer matrix. The high-frequency cavitation effect effectively breaks up particle agglomerates, ensuring a more uniform suspension and facilitating deeper infiltration of the PCL into the microgrooves of the SS 316L substrate surface (Fadli et al., 2023). This improved dispersion and penetration strengthen the mechanical interlocking at the coating-substrate interface, thereby increasing shear resistance. In addition, controlled drying conditions contribute to effective solvent evaporation and consolidation of the polymer matrix. This promotes densification of the coating layer, minimizes porosity, and reinforces the structural integrity of the composite film (Tirumkudulu & Punati, 2022). The interfacial adhesion is further supported by multiple bonding mechanisms, including hydrogen bonding, electrostatic interactions, and physical anchoring. These synergistic interactions collectively result in a robust and adherent coating structure. Optimizing these processing parameters significantly enhances not only the surface morphology but also the mechanical stability of the coating under physiological and load-bearing conditions (Ma et al., 2022). As a result, the PCL/HA composite coatings exhibit strong potential for orthopedic applications where durable implant-tissue integration and long-term interfacial integrity are essential (Shamsi et al., 2024).

To evaluate the adequacy of the model developed for predicting adhesive strength, a regression analysis was conducted using JMP Pro 14 software (SAS Institute Inc., 2018). As illustrated in Figure 2, the regression plot compares the actual adhesive strength values against the predicted values generated by the model. The observed points closely follow the diagonal line, indicating strong agreement between experimental and predicted data. The model achieved a high coefficient of determination (R^2) of 0.97, signifying that 97% of the variation in adhesive strength can be explained by the selected process parameters. Additionally, the Root Mean Square Error (RMSE) was 9.34 MPa, suggesting minimal deviation between predicted and observed responses. These results demonstrate that the linear model provides a satisfactory fit to the experimental data. Although a formal lack of fit test could not be performed due to the absence of replicate data, the strong R^2 and low RMSE values indicate that the model is adequate for predicting adhesive strength within the studied range. Future work may include replicate runs or center points to enable a statistical lack-of-fit test and assess potential curvature or higher-order interactions.

The regression plot reveals a strong alignment between the actual and predicted values of adhesive strength, closely following a linear trend line. This visual correlation confirms that the model effectively captures the relationship between the process parameters and the adhesive strength response. The proximity of the data points to the line of equality ($Y_{\text{actual}} = Y_{\text{predicted}}$) indicates minimal deviation and affirms the model's predictive reliability. A key metric supporting this observation is the coefficient of determination (R^2), which quantifies the proportion of variance in adhesive strength that can be explained by the independent variables: sonication temperature, PCL/HA ratio, and drying time. With an R^2 value approaching 1, the model demonstrates a high level of explanatory power, indicating that the selected variables significantly influence the adhesive strength. The high R^2 value obtained in this analysis confirms the model's adequacy in representing the experimental data and highlights its potential for guiding process optimization.

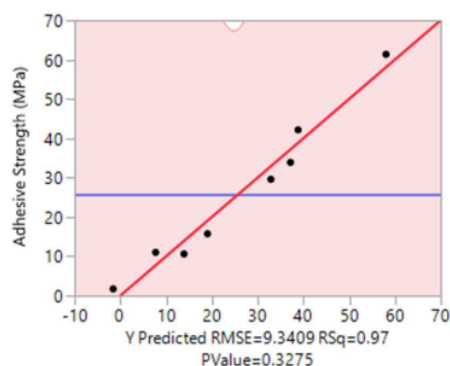


Figure 2. Regression plot of the predicted versus actual adhesive strength values.

The regression plot demonstrates that the actual and predicted values of adhesive strength are closely aligned along a linear trend, indicating that the model generally captures the response behavior well. This visual correspondence is further supported by the coefficient of determination (R^2) of 0.97, suggesting that 97% of the variability in adhesive strength can be explained by the selected process variables—namely, sonication temperature, PCL/HA ratio, and drying time. However, the adjusted R^2 value of 0.77 indicates a notable drop compared to R^2 , which may suggest potential overfitting or that some predictors contribute less meaningfully to the model once the number of terms is accounted for. The difference of 0.20 between R^2 and adjusted R^2 approaches the upper limit of what is generally considered acceptable, thus warranting careful interpretation. While the model fits the current data well, its ability to generalize may be limited without further validation. Additionally, the model's Root Mean Square Error (RMSE) of 9.34 MPa reflects moderate average deviations between predicted and observed values, which supports the model's predictive accuracy within the given range. The p-value of 0.3275, though not statistically significant at the 0.05 level, does not necessarily undermine the model, especially in the absence of replicate data, which limits formal lack-of-fit testing. Overall, while the model demonstrates strong visual and statistical fit to the experimental data, the relatively large gap between R^2 and adjusted R^2 highlights the need for model simplification or validation through additional experiments, potentially involving replicates or center points to assess robustness and reduce uncertainty.

Commented [r4]: just delete it

Table 3. Fit Statistic summary

R^2	0.968
R^2 Adj	0.777
Root Mean Square Error	9.34
Mean of Response	25.76 3682
p-Value	0.3275

The model selected is a linear model with interaction terms, constructed based on a full factorial 2^3 design. To evaluate the adequacy of the model, an Analysis of Variance (ANOVA) was conducted, with results summarized in Table 4. ANOVA serves multiple purposes in this context: it quantifies the overall significance of the model, assesses the contributions of individual variables and their interactions, and evaluates the model's ability to explain the variability of the adhesive strength response. The ANOVA results indicate that the overall model is not statistically significant, with a p-value of 0.3275, which is higher than the commonly accepted threshold of 0.05. This suggests that, based on the available data and degrees of freedom, there is insufficient statistical evidence to confirm that the model provides a meaningful explanation of the variation in adhesive strength. Furthermore, none of the individual terms—including the main effects (X1, X2, X3) and their interactions—exhibited statistical significance, with all p-values exceeding 0.05. Despite the lack of statistical significance, the model still shows a relatively high coefficient of

Commented [r5]:
Paragraphs are simplified to be more concise, concise and clear

determination ($R^2 = 0.97$), indicating a good fit to the observed data. However, the adjusted R^2 value of 0.77 suggests that this fit may be somewhat overstated due to the number of predictors relative to the sample size, potentially pointing to overfitting. The absence of replicates also limits the ability to perform a formal lack-of-fit test and to accurately estimate pure experimental error. While the statistical indicators imply that caution should be exercised in interpreting the model, the observed trends remain physically meaningful and align with expected experimental behavior. Future studies that incorporate replicated runs or center points are recommended to improve statistical reliability and enable more robust model validation. Similar considerations were highlighted by Fern and Salimi (2021), who emphasized the importance of statistical rigor and replication when constructing predictive models involving multiple interaction terms.

Commented [r6]: Paragraphs are simplified to be more concise, concise and clear

Table 4. ANOVA Summary for the Linear Interaction Model of Adhesive Strength

Source	Sum of Squares	df	Mean Square	F-value	p-value
Model	2654.06	6	442.34	5.06	0.3275
X1	537.9200	1		6.1651	0.2437
X2	1049.2781	1		12.0258	0.1787
X3	46.8512	1		0.5370	0.5974
X1*X2	0.0313	1		0.0004	0.9880
X1*X3	1010.7008	1		11.5837	0.1819
X2*X3	9.2880	1		0.1065	0.7992
Error	87.25	1	87.25		
Cor Total	2741.31	7			

In the statistical analysis of the adhesive strength response, the significance of individual model terms was assessed using the F-value and corresponding p-value ($\text{Prob} > F$), as presented in Table 4. The p-value indicates the probability that the observed effects are due to random variation rather than a true relationship between the input factors and the response. A term is typically considered statistically significant if its p-value is less than 0.05, indicating a less than 5% chance that the observed effect occurred randomly. Based on the ANOVA results, however, the overall model is not statistically significant, with an F-value of 5.06 and a model p-value of 0.3275, which exceeds the conventional 0.05 threshold. This suggests that the model, as formulated, may not reliably explain the variability in adhesive strength. Furthermore, none of the individual model terms—including the main effects (X1: sonication temperature, X2: PCL/HA ratio, X3: drying time) and their two-way interactions—were statistically significant, as all p-values were greater than 0.05. Although statistical significance was not achieved, regression modeling remains a valuable tool for exploring potential trends and guiding experimental optimization (Montgomery, 2017). In this study, the regression model was constructed using coded variables, where each level of a factor is standardized (e.g., -1, 0, +1). This approach facilitates comparison of the relative contributions of different variables to the response. While the model demonstrated a high coefficient of determination ($R^2 = 0.97$), the lower adjusted R^2 (0.77) and lack of statistical significance suggest that further refinement—such as increasing the number of replicates or expanding the design space—is necessary to improve model robustness and confirm factor significance.

Commented [r7]: Paragraphs are simplified to be more concise, concise and clear

The resulting model is presented in the form of a linear equation with interaction terms, which effectively predicts the adhesive strength based on the specified factor levels. The coded regression coefficients reflect the magnitude and direction of the effect that each variable exerts on the response. These coefficients are especially useful for identifying the most influential parameters and for guiding further optimization strategies. The complete coded model equation is given in Equation (1).

$$Y = 25.76 + 8.2X_1 + 11.4525X_2 + 2.42X_3 + 0.0625X_1X_2 + 11.24X_1X_3 - 1.0775X_2X_3 \dots \dots \dots (1)$$

Regression analysis is a fundamental statistical approach used to quantify the relationship between a dependent variable (response) and one or more independent variables (factors). In this study, regression was employed to model the influence of process variables—sonication temperature (X1), PCL/HA ratio (X2), and drying time (X3)—on the adhesive strength of the PCL/HA composite coating. A key component of regression diagnostics is the analysis of residuals, which are defined as the differences between the observed (actual) response values and the values predicted by the model. Ideally, residuals should be randomly distributed and centered

around zero, indicating that the model has effectively captured the underlying trend without systematic bias. This predictive model illustrates not only the main effects of each factor but also the interaction effects between them. For instance, the interaction between sonication temperature and drying time (X_1X_3) displays a relatively strong coefficient (+11.24), suggesting a synergistic influence on adhesive strength when both variables are increased concurrently. Conversely, the negative coefficient for the X_2X_3 interaction (-1.0775) implies a slight antagonistic effect between the PCL/HA ratio and drying time under certain conditions. To further explore these relationships, both interaction plots and three-dimensional response surface plots were generated. These visualizations provide insight into how the simultaneous variation of two factors influences the response while holding the third constant. Such graphical interpretation aids in understanding complex interactions, identifying optimal process conditions, and supporting the validation of the regression model's assumptions.

Commented [r8]: Paragraphs are simplified to be more concise, concise and clear

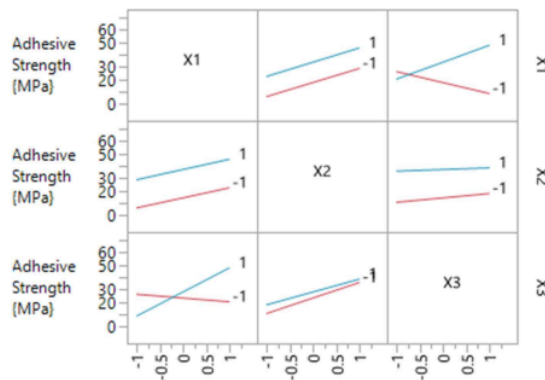


Figure 3. Interaction Plot for adhesive strength as a Function of X_1 , X_2 , and X_3

Figure 3 presents the interaction plots illustrating the combined effects of the process parameters—sonication temperature (X_1), PCL/HA ratio (X_2), and drying time (X_3)—on the adhesive strength of the PCL/HA composite coating. In these plots, the X-axis represents the coded levels of one variable (-1, 0, +1), while the Y-axis denotes the corresponding adhesive strength response in megapascals (MPa). The presence of an interaction is inferred when the response lines corresponding to different levels of the second variable are not parallel, indicating that the effect of one variable depends on the level of the other. A prominent interaction is observed between X_1 (sonication temperature) and X_2 (PCL/HA ratio). As both variables increase simultaneously, there is a significant enhancement in adhesive strength, suggesting a positive synergistic effect. This synergy could be attributed to improved dispersion of hydroxyapatite particles and enhanced polymer infiltration into the substrate surface, which are both facilitated by elevated sonication temperatures and optimized PCL/HA composition. The interaction between X_1 (sonication temperature) and X_3 (drying time) also demonstrates a notable increase in adhesive strength when both factors are at their higher levels. The divergence of the lines here indicates that the effect of drying time on adhesion is intensified at elevated sonication temperatures, possibly due to improved matrix densification and moisture elimination, which promote stronger interfacial bonding during curing. In contrast, the interaction between X_2 (PCL/HA ratio) and X_3 (drying time) appears relatively weaker, as indicated by the near-parallel nature of the response lines. This suggests that the adhesive strength is less sensitive to the simultaneous variation of these two parameters, or that their effects are mostly additive rather than interactive within the studied range. Overall, these interaction plots highlight the importance of optimizing multiple parameters simultaneously to maximize adhesive strength. The findings underscore that the combined influence of process parameters can have a greater impact than their individual contributions alone, a concept critical in the design of high-performance bioactive coatings.

Commented [r9]: Paragraphs are simplified to be more concise, concise and clear

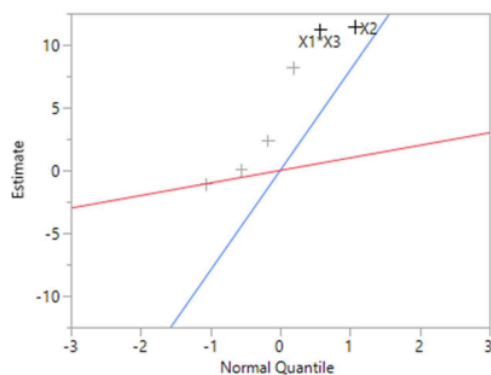


Figure 4. Normal probability plot of standardized effects for adhesive strength. Effects that deviate significantly from the reference line indicate significant contributions to the response.

Figure 4 presents the normal probability plot of standardized effects for the adhesive strength response of PCL/HA coatings. This graphical tool is used to identify significant factors and interactions in a factorial experiment by plotting the effect estimates against a theoretical normal distribution. Effects that lie far from the fitted reference line (red) are considered statistically significant, while those that lie close to the line are likely to be the result of random variation. In this plot, the effects of X_2 (PCL/HA ratio) and the interaction term $X_1 \cdot X_3$ (sonication temperature \times drying time) are the most prominent, lying farthest from the reference line. This indicates that both have a statistically significant influence on the adhesive strength of the coating. The strong contribution of X_2 suggests that the PCL/HA ratio plays a critical role in determining the bonding characteristics of the composite layer, possibly due to changes in polymer phase continuity or interfacial contact with the substrate. The significance of the $X_1 \cdot X_3$ interaction implies that the simultaneous adjustment of sonication temperature and drying time exerts a non-linear effect on adhesive strength. This could be explained by improved nanoparticle dispersion at higher sonication temperatures coupled with better matrix densification during extended drying—synergistically enhancing interfacial adhesion. In contrast, other main effects and interactions lie close to the reference line, suggesting they are statistically insignificant within the 95% confidence interval. These include the main effect of X_1 (sonication temperature), X_3 (drying time), and other interaction terms, which do not substantially impact the adhesive strength when considered independently or in combination within the studied range. This normal plot serves as a useful visual confirmation of the ANOVA findings and supports a focus on optimizing X_2 and the $X_1 \cdot X_3$ interaction for improving coating adhesion. Future experiments might benefit from a more refined exploration of these factors using response surface methodology to determine the optimal parameter window for maximum adhesive strength.

Commented [r10]: Paragraphs are simplified to be more concise, concise and clear

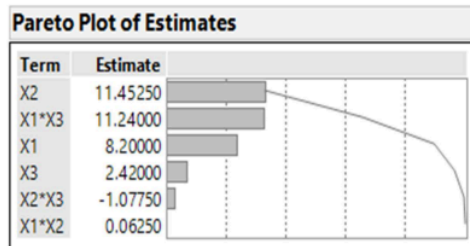


Figure 5. Pareto plot of estimates showing the relative contribution of each factor and interaction term to the adhesive strength of PCL/HA coatings.

The Pareto plot of standardized estimates shown in Figure 5 provides a visual representation of the relative importance of each factor and interaction term in influencing the adhesive strength of the PCL/HA coating. In this chart, the length of each bar corresponds to the absolute magnitude of the term's effect estimate, with larger bars indicating greater impact on the response variable. From the plot, it is evident that the PCL/HA ratio (X_2) has the most significant positive effect on adhesive strength, with an estimated contribution of 11.45 MPa. This suggests that optimizing the PCL/HA ratio is critical in enhancing the interfacial bonding between the coating and the stainless steel substrate. The interaction term $X_1 \cdot X_3$ (sonication temperature \times drying time) also shows a substantial effect (11.24 MPa), highlighting that the combination of these two parameters synergistically improves the adhesive strength. This may be attributed to the fact that appropriate sonication can enhance particle dispersion, while suitable drying time promotes uniform film formation and better adhesion. The main effect of sonication temperature (X_1) follows next, with a notable positive influence of 8.2 MPa, indicating that increasing the sonication temperature contributes to stronger coating-substrate adhesion, likely due to improved nanoparticle distribution and interfacial interaction. The drying time (X_3) shows a moderate effect (2.42 MPa), suggesting its role in solvent evaporation and final film consolidation. While $X_2 \cdot X_3$ has a negative effect (-1.07 MPa), indicating a potentially antagonistic interaction between PCL/HA ratio and drying time, the $X_1 \cdot X_2$ interaction appears negligible (0.06 MPa) and likely not statistically significant.

Commented [r11]: Paragraphs are simplified to be more concise, concise and clear

The three-dimensional response surface plots presented in Figures 6 illustrate the interaction effects of process parameters—sonication temperature (X_1), PCL/HA ratio (X_2), and drying time (X_3)—on the adhesive strength of PCL/HA composite coatings applied to 316L stainless steel substrates. These plots help visualize the combined influence of two variables at a time, while holding the third variable at its central level, thus allowing for interpretation of interaction effects critical to coating adhesion performance. As shown in Figure 8a, the interaction between sonication temperature (X_1) and PCL/HA ratio (X_2) has a significant influence on the adhesive strength. The surface exhibits a rising gradient from lower-left to upper-right, forming a planar and positively sloped surface. This trend indicates a synergistic effect where increasing both parameters simultaneously leads to a noticeable improvement in adhesive strength. The consistent elevation suggests that these variables contribute additively rather than interactively in a nonlinear manner. Higher sonication temperatures may enhance particle dispersion and interfacial bonding, while an increased PCL/HA ratio likely promotes better matrix continuity—both contributing to enhanced adhesion.

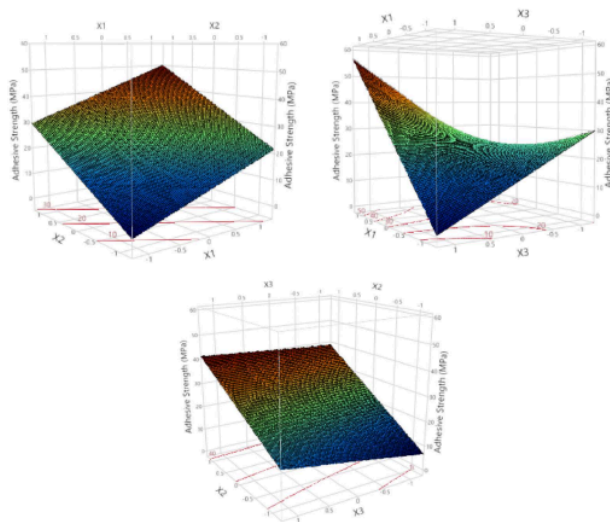


Figure 6. Three-dimensional response surface plots illustrating the interaction effects of (a) sonication temperature and PCL/HA ratio, (b) sonication temperature and drying time, and (c) PCL/HA ratio and drying time on the adhesive strength of PCL/HA-coated stainless steel.

Figure 6b presents the interaction between sonication temperature (X_1) and drying time (X_3). This surface displays a non-linear, saddle-like curvature with a peak in adhesive strength observed when the sonication temperature is high and the drying time is low. Conversely, low temperature combined with prolonged drying yields reduced adhesive strength. This interaction suggests that while moderate to high sonication temperature improves nanoparticle dispersion and matrix infiltration, extended drying time may reduce bonding efficacy due to potential microcracking or shrinkage stress during solvent evaporation. Therefore, the optimal adhesion is achieved through a precise balance between sufficient particle dispersion and controlled drying kinetics. In Figure 6c, the interaction between PCL/HA ratio (X_2) and drying time (X_3) shows a moderately curved surface, with adhesive strength decreasing as both variables increase. The surface trend indicates a negative synergistic effect, where increasing either parameter beyond a threshold leads to a reduction in adhesion performance. This could be due to a higher PCL content forming a less rigid matrix that reduces interfacial grip, and longer drying times potentially leading to brittle or poorly consolidated structures. Hence, a careful balance between polymer concentration and drying duration is essential for maximizing adhesive performance. Taken together, the response surface analysis highlights that the adhesive strength of PCL/HA coatings is strongly influenced by both individual parameters and their interactions. While sonication temperature and PCL/HA ratio exhibit synergistic enhancement, the drying time must be carefully controlled to avoid undermining the adhesion benefits gained from the other two variables.

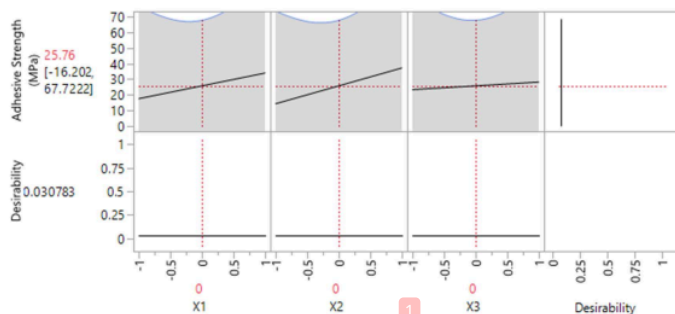


Figure 7. Desirability profiler showing the effects of sonication temperature (X_1), PCL/HA ratio (X_2), and drying time (X_3) on predicted adhesive strength and overall desirability.

The desirability profiler in Figure 7 illustrates the influence of three key process variables—sonication temperature (X_1), PCL/HA ratio (X_2), and drying time (X_3)—on the predicted adhesive strength of the composite coating and its corresponding desirability score. The top panel of the profiler displays the predicted adhesive strength values (in MPa) along with 95% confidence intervals, while the bottom panel represents the desirability values ranging from 0 (least desirable) to 1 (most desirable), which reflect the optimization target. The trend for X_1 (sonication temperature) reveals a moderate positive effect on adhesive strength. As the temperature increases, the enhanced dispersion of HA particles and improved polymer penetration into the substrate surface likely contribute to stronger interfacial adhesion. Similarly, X_2 (PCL/HA ratio) also shows a rising response, indicating that increasing the PCL content improves the mechanical integrity of the coating layer by increasing polymer flexibility and cohesive bonding. However, X_3 (drying time) demonstrates a negative slope, suggesting that prolonged drying might lead to brittleness, shrinkage, or the formation of microcracks. These defects weaken the mechanical bonding between the coating and substrate, leading to reduced adhesive performance. Despite these observed trends, the overall desirability score remains very low, with a value of 0.03, and the predicted optimized adhesive strength is only 25.76 MPa. This result indicates that the current combination of factor levels does not sufficiently meet the desired adhesive performance target. The low desirability function implies either the optimization constraints were too stringent or the response surface is inherently limited under the selected parameter range. From a process control standpoint, this outcome highlights the need for further exploration of process windows. Adjustments such as increasing the upper limit of sonication temperature or optimizing post-processing conditions (e.g., curing or crosslinking techniques) may be necessary to significantly enhance the adhesive strength. As it stands, although certain trends are favorable, the predicted performance remains suboptimal, underscoring the need for refinement in parameter selection and model re-evaluation to reach clinically relevant adhesion thresholds for biomedical implant applications.

Commented [r12]: Paragraphs are simplified to be more concise, concise and clear and make one paragraph

4. Conclusion

This study successfully demonstrated the influence of three key process variables—sonication temperature, PCL/HA ratio, and drying time—on the adhesive strength of PCL/HA composite coatings applied to 316L stainless steel via the dip-coating method. Statistical modeling and response surface analysis revealed that sonication temperature and PCL/HA ratio had the most significant positive impact on the bonding performance, enhancing the interfacial adhesion between the coating and the metal substrate. In contrast, extended drying time had a detrimental effect, likely due to film shrinkage, microcracking, or reduced interfacial cohesion. Interaction plots and Pareto analysis supported the dominance of PCL/HA ratio and sonication temperature in determining adhesive strength outcomes. The optimization model predicted a maximum

adhesive strength of 25.76 MPa, albeit with a low desirability score (0.03), indicating the challenge in fine-tuning all parameters to achieve optimal bonding performance. These findings highlight the importance of controlling process conditions to enhance coating adhesion, offering valuable insights for the development of mechanically robust bioactive coatings for biomedical implant applications.

References

Commented [r13]: Reference used Mendeley tools

15. Aroussi, D., Aour, B., & Bouaziz, A. S. (2019). A Comparative Study of 316L Stainless Steel and a Titanium Alloy in an Aggressive Biological Medium. *Engineering, Technology & Applied Science Research*, 9(6).
16. Drevet, R., Fauré, J., & Benhayoune, H. (2023). Bioactive calcium phosphate coatings for bone implant applications: a review. *Coatings*, 13(6), 1091.
17. Fadli, A., Yenti, S. R., Huda, F., Prabowo, A., & Marbun, U. N. (2021). Empirical model to predict the hydroxyapatite thickness on the surface of 316l stainless steel by the dip coating method. *Ceramics-Silikáty*, 65(4), 386-394.
18. Fadli, A., Prabowo, A., Utama, Panca setia, Aziz, Y., & Heltina, D. (2023). SIGNIFICANCE OF THE PCL CONCENTRATION ON THE ELECTROCHEMICAL AND MECHANICAL PERFORMANCE OF A PCL/HA COATING ON SS 316L. *Ceramics-Silikáty*, 67(4), 551-561.
19. Fern, H. W., & Salimi, M. N. (2021, May). Hydroxyapatite nanoparticles produced by direct precipitation method: Optimization and characterization studies. In *AIP Conference Proceedings* (Vol. 2339, No. 1, p. 020215). AIP Publishing LLC.
20. Gunatillake, P. A., & Adhikari, R. (2003). Biodegradable synthetic polymers for tissue engineering. *European Cells and Materials*, 5, 1-16.
21. Haleem, A. H., Radhi, N. S., Jaber, N. T., & Al-Khafaji, Z. (2024). Preparation and Exploration of Nano-Multi-Layers on 316L Stainless Steel for Surgical Tools. *Jordan Journal of Mechanical & Industrial Engineering*, 18(2).
22. Hetemi, D., & Pinson, J. (2019). Functionalization of polymers by hydrolysis, aminolysis, reduction, oxidation, and some related reactions. *Surface Modification of Polymers: Methods and Applications*, 211-240.
23. Homa, K., Zakrzewski, W., Dobrzyński, W., Piszko, P. J., Piszko, A., Matys, J., ... & Dobrzyński, M. (2024). Surface functionalization of titanium-based implants with a nanohydroxyapatite layer and its impact on osteoblasts: a systematic review. *Journal of Functional Biomaterials*, 15(2), 45.
24. Huynh, V., Ngo, N., & Golden, T. (2019). Surface activation and pretreatments for biocompatible metals and alloys used in biomedical applications. *International Journal of Biomaterials*, 2019, 1-21. <https://doi.org/10.1155/2019/3806504>
25. Ielo, I., Calabrese, G., Luca, G., & Conoci, S. (2022). Recent advances in hydroxyapatite-based biocomposites for bone tissue regeneration in orthopedics. *International Journal of Molecular Sciences*, 23(17), 9721. <https://doi.org/10.3390/ijms23179721>
26. Liang, H. Y., Lee, W. K., Hsu, J. T., Shih, J. Y., Ma, T. L., Vo, T. T. T., ... & Lee, I. T. (2024). Polycaprolactone in bone tissue engineering: a comprehensive review of innovations in scaffold fabrication and surface modifications. *Journal of functional biomaterials*, 15(9), 243.
27. Luo, J., Jia, X., Gu, R., Peng, Z., Huang, Y., Sun, J., ... & Yan, M. (2018). 316l stainless steel manufactured by selective laser melting and its biocompatibility with or without hydroxyapatite coating. *Metals*, 8(7), 548. <https://doi.org/10.3390/met8070548>
28. Ma, X., Zhou, X., Ding, J., Huang, B., Wang, P., Zhao, Y., ... & Xu, W. (2022). Hydrogels for underwater adhesion: adhesion mechanism, design strategies and applications. *Journal of Materials Chemistry A*, 10(22), 11823-11853.

22

Monia, T., & Ridha, B. C. (2024). Polymer-ceramic composites for bone challenging applications: Materials and manufacturing processes. *Journal of Thermoplastic Composite Materials*, 37(4), 1540-1557.

Montgomery, D. C. (2017). *Design and Analysis of Experiments* (9th ed.). John Wiley & Sons

Ramesh, N., Moratti, S. C., & Dias, G. J. (2018). Hydroxyapatite-polymer biocomposites for bone regeneration: A review of current trends. *Journal of Biomedical Materials Research Part B: Applied Biomaterials*, 106(5), 2046-2057.

Saputra, A., Syafitri, U., Sudiro, T., Timuda, G., & Sari, Y. (2021). Gas pressure and coating distance for nanohydroxyapatite deposition on stainless steel 316L using flame spray technique. *Journal of Metals Materials and Minerals*, 31(1).

SAS Institute Inc. (2018). *JMP Pro 14 Statistical Discovery from SAS*. SAS Institute Inc.

Shamsi, M., Sedighi, M., & Bagheri, A. (2024). Surface modification of biodegradable Mg/HA composite by electrospinning of PCL/HA fibers coating: Mechanical properties, corrosion, and biocompatibility. *Transactions of Nonferrous Metals Society of China*, 34(5), 1470-1486.

Singh, J., Singh, J., Kumar, S., & Gill, H. (2023). Short review on hydroxyapatite powder coating for ss 316L. *Journal of Electrochemical Science and Engineering*, 13(1), 25-39.

Soriente, A., Fasolino, I., Sánchez, A., Prokhorov, E., Buonocore, G., Luna-Bárcenas, G., ... & Raucci, M. (2021). Chitosan/hydroxyapatite nanocomposite scaffolds to modulate osteogenic and inflammatory response. *Journal of Biomedical Materials Research Part A*, 110(2), 266-272.

Sowmya, B., Hemavathi, A. B., & Panda, P. K. (2021). Poly (ϵ -caprolactone)-based electrospun nano-featured substrate for tissue engineering applications: A review. *Progress in biomaterials*, 10(2), 91-117.

Taghizadeh, F., Heidari, M., Mostafavi, S., Mortazavi, S. M., & Haeri, A. (2024). A review of preparation methods and biomedical applications of poly (ϵ -caprolactone)-based novel formulations. *Journal of Materials Science*, 59(24), 10587-10622.

Tirumkudulu, M. S., & Punati, V. S. (2022). Solventborne polymer coatings: Drying, film formation, stress evolution, and failure. *Langmuir*, 38(8), 2409-2414.

Ulery, B. D., Nair, L. S., & Laurencin, C. T. (2011). Biomedical applications of biodegradable polymers. *Journal of Polymer Science Part B: Polymer Physics*, 49(12), 832-862.

Vasudev, H. and Prakash, C. (2023). Surface engineering and performance of biomaterials. *Journal of Electrochemical Science and Engineering*, 13(1), 1-3. <https://doi.org/10.5599/jese.1698>.

29. Adhesive Behavior of Polycaprolactone review 1.docx

ORIGINALITY REPORT

24%

SIMILARITY INDEX

21%

INTERNET SOURCES

20%

PUBLICATIONS

12%

STUDENT PAPERS

PRIMARY SOURCES

- | | | |
|---|---|----|
| 1 | www2.irsm.cas.cz
Internet Source | 4% |
| 2 | www.mdpi.com
Internet Source | 1% |
| 3 | Ahmad Fadli. "SIGNIFICANCE OF THE PCL CONCENTRATION ON THE ELECTROCHEMICAL AND MECHANICAL PERFORMANCE OF A PCL/HA COATING ON SS 316L.", Ceramics - Silikaty, 2023
Publication | 1% |
| 4 | Amran Hossain, Md Rifat Hossain Shuvo, Safiullah Khan, Abu Sad MD Sayem, Safiul Islam, Nayem Hossain. "Functional nanoparticle developments for 3D-printed biodegradable implants- A comprehensive review", Results in Surfaces and Interfaces, 2025
Publication | 1% |
| 5 | Hemant Kumar Pant, Amit Kumar Singh, T. Jagadeesha. "Chapter 6 Biodegradation | 1% |

Behavior of Magnesium-Based Biomaterials Using Surface Modification Techniques for Orthopedic Implants: A Review", Springer Science and Business Media LLC, 2025

Publication

6	Submitted to University of Wales Swansea Student Paper	1 %
7	revistademetalurgia.revistas.csic.es Internet Source	1 %
8	Cory Dian Alfarisi, Nurfatihayati, Hari Rionaldo, Ahmad Fadli et al. "The effect of acid treatment and sintering temperature on 316L stainless steel substrate coating with hydroxyapatite", Materials Today: Proceedings, 2023 Publication	1 %
9	biblio.cinvestav.mx Internet Source	1 %
10	Submitted to Queen Mary and Westfield College Student Paper	<1 %
11	Submitted to University of Nottingham Student Paper	<1 %
12	Anqi Xu, Nan Zhang, Shixing Su, Hongyu Shi et al. "A highly stretchable, adhesive, and antibacterial hydrogel with chitosan and	<1 %

tobramycin as dynamic cross-linkers for
treating the infected diabetic wound",
Carbohydrate Polymers, 2023

Publication

13

jmmm.material.chula.ac.th

Internet Source

<1 %

14

www.nsf.ac.lk

Internet Source

<1 %

15

repository.penerbiteureka.com

Internet Source

<1 %

16

de Sousa, Diogo Pereira. "Desenvolvimento de Estruturas Fibrosas 3D para Substituição de Tendões e Ligamentos.", Universidade do Minho (Portugal), 2024

Publication

<1 %

17

repo.undiksha.ac.id

Internet Source

<1 %

18

ouci.dntb.gov.ua

Internet Source

<1 %

19

pub.iapchem.org

Internet Source

<1 %

20

hrcak.srce.hr

Internet Source

<1 %

21

pmc.ncbi.nlm.nih.gov

Internet Source

<1 %

22	Submitted to Chandigarh Group of Colleges Student Paper	<1 %
23	dokumen.pub Internet Source	<1 %
24	mail.i-scholar.in Internet Source	<1 %
25	Stephanie Solal Djimtoingar, Nana Sarfo Agyemang Derkyi, Francis Atta Kuranchie. "OPTIMISATION OF THE ANAEROBIC CO-DIGESTION PROCESS OF CALOTROPIS PROCERA LEAVES, STEMS, AND COW DUNG USING A MIXTURE DESIGN", South African Journal of Chemical Engineering, 2023 Publication	<1 %
26	Submitted to University of Samarra Student Paper	<1 %
27	ebin.pub Internet Source	<1 %
28	idoc.pub Internet Source	<1 %
29	Submitted to Saxion Brightspace Student Paper	<1 %
30	doras.dcu.ie Internet Source	<1 %

31	Internet Source	<1 %
32	www.jurnal.unsyiah.ac.id Internet Source	<1 %
33	"Design and Modeling of Mechanical Systems - VI", Springer Science and Business Media LLC, 2024 Publication	<1 %
34	Submitted to University of Wollongong Student Paper	<1 %
35	Submitted to University of Central Oklahoma Student Paper	<1 %
36	Submitted to Northcentral Student Paper	<1 %
37	editorialmarcaribe.es Internet Source	<1 %
38	Submitted to Trinity College Student Paper	<1 %
39	hdl.handle.net Internet Source	<1 %
40	repository.bakrie.ac.id Internet Source	<1 %
41	umpir.ump.edu.my Internet Source	<1 %

42	Ahmad Fadli, Agung Prabowo, Silvia Reni Yenti, Febliil Huda, Ayla Annisa Liswani, Donda Lamsinar Br Hutaauruk. "High Performance Of Coating Hydroxyapatite Layer On 316L Stainless Steel Using Ultrasonically And Alkaline Pretreatment", Journal of King Saud University - Science, 2023 Publication	<1 %
43	Debasis Nayak, Biswajit Kumar Swain. "Surface Engineering of Biomaterials - Synthesis and Processing Techniques", CRC Press, 2024 Publication	<1 %
44	Submitted to Institute of Graduate Studies, UiTM Student Paper	<1 %
45	Maedeh Soleimani, Hamzeh Ali Jamali, Milad Mousazadehgavan, Reza Ghanbari. "Chromium adsorption using powdered leaves of Prosopis cineraria: Kinetic, isotherm, and optimization by response surface methodology", Desalination and Water Treatment, 2024 Publication	<1 %
46	Hadli A. Harahap, Tresna Dewi, Rusdianasari. "Automatic Cooling System for Efficiency and Output Enhancement of a PV System	<1 %

47

Pinar Cihan, Fatma Alfarra, H. Kurtulus Ozcan, Mirac Nur Ciner, Atakan Ongen. "Prediction of hydrogen and methane yields from gasification of leather waste using machine learning and explainable AI: An original dataset", Journal of Environmental Management, 2025

Publication

<1 %

48

repositorio.cinvestav.mx

Internet Source

<1 %

49

www.researchsquare.com

Internet Source

<1 %

50

Ahmad Fadli, Fransisca Kristin, Putri Arini, Wisrayeti, Silvia Reni Yenti, Rozanna Sri Irianty. "Hydroxyapatite Coating On 316L Stainless Steel Using Dip Coating Technique", Journal of Physics: Conference Series, 2021

Publication

<1 %

51

Hagar M. Mahdy, Hanan Hendawy, Yehia M. Abbas, El-shazly M. Duraia. "Design and characterization of AgVO₃-HAP/GO@PCL ceramic-based scaffolds for enhanced wound healing and tissue regeneration", Journal of Materials Science: Materials in Medicine, 2025

<1 %

-
- | | | |
|---|--|----------------|
| <div style="background-color: #00728f; color: white; display: inline-block; width: 40px; height: 40px; text-align: center; line-height: 40px; margin-bottom: 5px;">52</div> | <p>Jian Ma, Gang Xu, Kai Wu, Chengji Xu, Yu Liu, Nanxi Dang, Qiang Zeng, Qing Lü.
"Heterogeneous distribution of lightweight porous ceramic sands in a high strength cement grout", Construction and Building Materials, 2023</p> <p>Publication</p> | <p><1 %</p> |
|---|--|----------------|
-
- | | | |
|---|---|----------------|
| <div style="background-color: #008000; color: white; display: inline-block; width: 40px; height: 40px; text-align: center; line-height: 40px; margin-bottom: 5px;">53</div> | <p>Xiaodong Yu, Zhenfu Luo. "Spatial distribution characteristics of <1.5mm oil shale powder and its influence on the separation of low rank oil shale", Fuel, 2025</p> <p>Publication</p> | <p><1 %</p> |
|---|---|----------------|
-
- | | | |
|---|---|----------------|
| <div style="background-color: #d4af37; color: white; display: inline-block; width: 40px; height: 40px; text-align: center; line-height: 40px; margin-bottom: 5px;">54</div> | <p>epdf.pub</p> <p>Internet Source</p> | <p><1 %</p> |
|---|---|----------------|
-
- | | | |
|---|---|----------------|
| <div style="background-color: #8b4513; color: white; display: inline-block; width: 40px; height: 40px; text-align: center; line-height: 40px; margin-bottom: 5px;">55</div> | <p>ia802507.us.archive.org</p> <p>Internet Source</p> | <p><1 %</p> |
|---|---|----------------|
-
- | | | |
|---|---|----------------|
| <div style="background-color: #003366; color: white; display: inline-block; width: 40px; height: 40px; text-align: center; line-height: 40px; margin-bottom: 5px;">56</div> | <p>journals.lww.com</p> <p>Internet Source</p> | <p><1 %</p> |
|---|---|----------------|
-
- | | | |
|---|--|----------------|
| <div style="background-color: #800080; color: white; display: inline-block; width: 40px; height: 40px; text-align: center; line-height: 40px; margin-bottom: 5px;">57</div> | <p>Marco Domingos, Antonio Gloria, Jorge Coelho, Paulo Bartolo, Joaquim Ciurana.
"Three-dimensional printed bone scaffolds: The role of nano/micro-hydroxyapatite particles on the adhesion and differentiation of human mesenchymal stem cells",
Proceedings of the Institution of Mechanical</p> | <p><1 %</p> |
|---|--|----------------|

Engineers, Part H: Journal of Engineering in Medicine, 2017

Publication

58

espace.curtin.edu.au

Internet Source

<1 %

59

nano-ntp.com

Internet Source

<1 %

60

İbrahim Yasin Köktaş, Ömür Gökkuş, İshak Afşin Kariper, Amina Othmani. "Tetracycline removal from aqueous solution by electrooxidation using ruthenium-coated graphite anode", Chemosphere, 2023

Publication

<1 %

61

Bo Ding, Ming Ding, Yangzhou Ma, Guangsheng Song, Zongqun Li, Jinlong Ge, Weidong Yang, Cuie Wen. "Effect of MgO on electrochemical properties of silicon-based anode composite material", Solid State Sciences, 2022

Publication

<1 %

62

Jinchao Li, Wei Zhang, Hongyu Zheng, Jun Gao, Chao Jiang. "Reducing plasma shielding effect for improved nanosecond laser drilling of copper with applied direct current", Optics & Laser Technology, 2023

Publication

<1 %

63	Pushpa Choudhary, Sambit Satpathy, Arvind Dagur, Dharendra Kumar Shukla. "Recent Trends in Intelligent Computing and Communication", CRC Press, 2025 Publication	<1 %
64	Smith, . "4. Designs for Simplex-Shaped Regions", Experimental Design for Formulation, 2005. Publication	<1 %
65	etasr.com Internet Source	<1 %
66	progressinorthodontics.springeropen.com Internet Source	<1 %
67	repositorio.ufrn.br Internet Source	<1 %
68	repository-tnmgrmu.ac.in Internet Source	<1 %
69	www.gecekitapligi.com Internet Source	<1 %
70	www.grafiati.com Internet Source	<1 %
71	www.irsm.cas.cz Internet Source	<1 %
72	Noémi Izabella Farkas, Réka Barabás, Graziella Liana Turdean, Liliana Bizo.	<1 %

"Investigation of optimized poly(lactic acid)/hydroxyapatite/doxycycline coatings on titanium alloy surfaces", Materials Science and Engineering: B, 2025

Publication

73

B. Sowmya, P. K. Panda. "Fabrication and characterization of super-hydrophilic poly (ε-caprolactone)/hydroxypropyl methylcellulose (HPMC) based composite electrospun membranes for tissue engineering applications", Progress in Biomaterials, 2022

Publication

<1 %

Exclude quotes Off

Exclude matches Off

Exclude bibliography Off